

Positron Binding and Annihilation Properties of Amino Acid Systems

Maya Ozaki,* Daisuke Yoshida,* Yukiumi Kita,* Tomomi Shimazaki,* and Masanori Tachikawa*

Cite This: *ACS Omega* 2021, 6, 29449–29458

Read Online

ACCESS |



Metrics & More

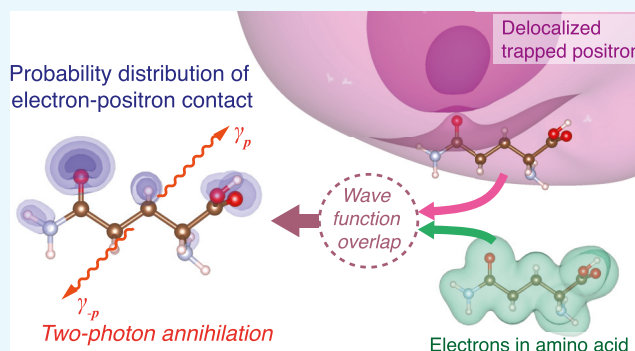


Article Recommendations



Supporting Information

ABSTRACT: Despite the fact that the positron annihilation has been used in biomedical applications, the detailed mechanism of the positron annihilation on biological molecules remains poorly understood so far. In this work, we investigated the positron binding and positron annihilation properties for both global minimum and hydrogen-bonded structures of 20 amino acid molecules using the multicomponent molecular orbital method. By regression analysis, we confirmed that positron affinity can increase with an increase of the permanent dipole moment of the parent amino acids as reported in previous studies, while the annihilation rate linearly increases with respect to the square root of positron affinity. By the one-particle property analyses for probabilities of electron–positron contacts, we found that delocalization characteristics of both electrons and positrons play key roles to enhance the positron annihilation rate arising from both the valence electrons in σ - and π -type molecular orbitals from 2p atomic orbitals but not from the highest occupied molecular orbital electrons, particularly for comparatively weakly bound positronic amino acid systems.



INTRODUCTION

Positron annihilation has been versatily used in many fields of materials science and biomedical science as a useful and versatile tool for a noninvasive probe of material properties and molecular processes. In bulk materials, positron annihilation occurs in the region of negatively charged defects or vacancy defects, which gives us various detailed properties of bulk defects.¹ For molecular systems, a positron can be trapped in the (induced) electronic dipole field of even neutral molecules. In biomedical fields, positron emission tomography as an important medical application has been used for cancer detection,^{2,3} where techniques of detection of γ -rays emitted upon electron–positron pair annihilation⁴ are used. Therefore, it is necessary to figure out the electron–positron pair annihilation properties as well as the positron binding ability of individual biological molecules.

For some isolated atoms, reliable theoretical calculations have provided theoretical evidence for the existence of a positronic bound state.^{5–8} On the other hand, in recent years, low-energy positron beam experimental studies by Surko's group have identified positron–molecule bound states and observed positron annihilation spectra for a number of individual molecules, containing small inorganic molecules and typical polyatomic organic molecules.^{9–14} From these theoretical and experimental results, some important trends for the capability of positron binding have been determined: the ionization energy of the parent atom becomes a key parameter for the positron binding energies of, for example, alkali-metal atoms, as described

by the alkali model proposed by Mitroy et al.,¹⁵ where the electron removal energy for the parent species in comparison to the binding energy of the positronium atom characterizes stabilities of the positron–atomic systems associated with the positronium or the positron decay channel. This trend is also likely to hold for a few aromatic compounds.¹⁶ In contrast, in the case of large organic molecules as represented by large alkane species, the positron binding energy can increase independently of the ionization energy, i.e., behaves like a constant with respect to the ionization energy.¹⁶ Gribakin et al. also have presented the important relationship between the positron binding energy and the electrostatic properties of the parent molecule, such as the permanent dipole moment and the dipole polarizability.¹⁶

On the theoretical side, direct calculations have also been performed to provide positron binding energies for positronic compounds of various sizes of molecules. In practice, highly accurate calculation methods to include a significant interparticle correlation effect, such as the configuration interaction method,^{17–23} more sophisticated quantum Monte Carlo method,^{24–26} and correlated Gaussian expansion approach,²⁷

Received: June 29, 2021

Accepted: October 14, 2021

Published: October 27, 2021



Table 1. Dipole Moments μ in debye, Positron Affinities PA in meV, and Annihilation Rates Γ_2 in ns⁻¹ for Positronic Amino Acid Systems Obtained by the Present MC_MO HF Calculations

species	Charry et al. ³⁸			this work			
	μ (Debye)	PA ^a (meV)	PA ^b (meV)	μ (debye)	PA ^c (meV)	Γ_2^{HF} (10 ⁻² ns ⁻¹)	Γ_2 (10 ⁻² ns ⁻¹)
Global Minimum Structures							
Gln	3.61	0.9	2.3	3.62	1.86	0.169	0.714
His	4.89	4.8	7.0	3.64	7.42	0.289	1.358
Ser	2.88	-0.2	0.8	1.69	-5.30		
Trp	1.19	-1.8	-1.7	4.13	2.44	0.122	0.519
Hydrogen Bonded Structures							
Ala	5.60	52.9	103.2	5.40	42.48	1.216	4.794
Arg	7.40	70.6	129.3	6.54	64.23	1.694	6.640
Asn	4.69	16.9	39.7	4.48	12.98	0.440	1.770
Asp	4.54	18.0	41.4	4.36	13.73	0.443	1.774
Cys	4.13	14.8	38.1	3.97	10.63	0.418	1.693
Gln	6.28	47.8	93.2	5.33	27.82	0.855	3.369
Glu	6.55	62.8	115.4	6.39	57.10	1.411	5.432
Gly	5.76	57.3	105.5	5.57	48.99	1.315	5.154
His	3.13	3.1	13.3	4.02	6.25	0.283	1.159
Ile	5.48	48.7	104.2	5.39	43.77	1.385	5.474
Leu	5.74	58.1	117.2	5.57	51.41	1.534	6.038
Lys	4.40	36.3	84.8	5.72	51.19	1.496	5.884
Met	4.45	30.1	72.0	6.52	58.30	1.416	5.514
Phe	5.61	50.6	107.5	5.40	42.84	1.309	5.162
Pro	6.03	72.0	138.4	5.75	59.78	1.733	6.816
Ser	4.31	9.3	21.6	4.39	19.22	0.645	2.580
Thr	4.43	11.5	27.0	4.45	19.28	0.700	2.798
Trp	7.08	79.4	153.4	6.03	57.77	1.680	6.593
Tyr	4.97	41.0	91.9	3.71	7.62	0.492	1.983
Val	5.31	42.3	91.3	5.07	30.23	0.958	3.806

^aAPMO HF calculation results. ^bAPMO P2 calculation results. ^cThe present MC_MO HF calculation results.

can be applied for rather positronic atoms or positronic small polyatomic systems due to these becoming computationally demanding. Theoretical studies also have now developed effective model potential methods with a focus on the positron binding interaction to the nonpolar or weakly polar systems.^{28,29} On the other hand, the mean-field Hartree–Fock (HF) level of the theory severely underestimates the positron affinity (PA) as well as the electron–positron pair annihilation rate due to incomplete interparticle correlation effects, e.g., in case studies for positronic polar molecules, such as cyanide species²² and alkali-metal halides,²⁶ the HF method can reproduce ~10% of PAs compared to the experimental or higher accuracy calculation results. However, the HF method of the multi-component molecular orbital (MC_MO) theory has been frequently applied for systematic studies, particularly for large sizes of polyatomic molecules^{30,31} and molecular clusters,³² which have not been experimentally identified.

For biological molecules, in contrast to the typical organic molecules, there was previously only an experimental report on positron lifetime observations for solid-phase amino acids and proteins.³³ In more recent years, a few theoretical investigations for the positron binding properties of the gas-phase amino acid molecules were performed using the MC_MO-based HF method. Koyanagi et al.³⁴ systematically investigated the positronic bound states of several amino acid species in the gas phase and successfully expected that the amino acids can have greater positive PAs as the molecular dipole moment increases. Furthermore, Nummela et al.³⁵ and Suzuki et al.³⁶ presented the hydration effect on positron binding to the aqueous complexes of glycine and proline, respectively, through

detailed analyses of the positron binding properties for a number of possible lowest energy conformers. Sugiura et al. carried out the simulation of the positron scattering on a proline molecule and obtained the positron annihilation spectrum containing vibrational resonance peaks.³⁷ On the other hand, Charry et al. also carried out calculations of PAs for amino acids³⁸ using any particle molecular orbital (APMO) method,³⁹ which is a similar approach to MC_MO. APMO-based second-order Møller–Plesset and second-order propagator calculations significantly improved underestimations of the HF level calculations for PA by taking into account the electron–positron correlation effect.³⁸ These high-level calculations as well as the above HF calculation results also showed that a linear trend on PA with respect to the dipole moment of the parent molecule holds good. These facts offer us a significant prediction that at least observables as the positron affinity and the positron annihilation rate should be observed as larger values than expectations from the HF level calculations. Although the positron binding abilities and the annihilation properties have become clear only for particular species, there are still neither available experimental data nor systematic theoretical benchmarks for the positron annihilation rates of the individual positronic compounds of the biological molecular systems. Therefore, it would be a very important step to find out chemical trends from theoretical benchmarks for the positron annihilation rate of the biological molecules in the MC_MO HF approach.

In particular, for some simple molecular systems, such as noble gas atoms, diatomic molecules, and typical hydrocarbons, the HF method has also been applied to evaluate the electron–positron annihilation spectra and utilized to understand the

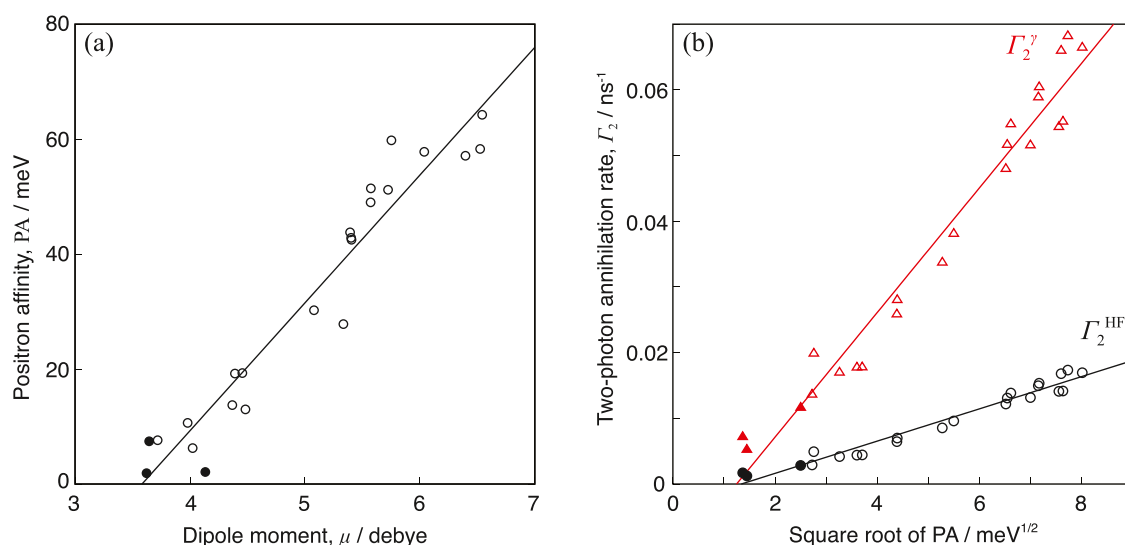


Figure 1. (a) Positron affinity PA (in meV) as a function of the magnitude of the dipole moment μ (in debye) of the parent amino acid molecule and (b) two-photon annihilation rates, Γ_2^{HF} and Γ_2^{γ} (in ns⁻¹), as functions of the square root of PA for positronic compounds of the amino acid molecules. Both PA and Γ_2^{HF} calculated directly by MC_MO HF calculations are shown by black circles, and Γ_2^{γ} including corrections by the enhancement factor is shown by red triangles, where for both figures, open and closed symbols indicate results for HB and GM structures, respectively. Solid lines are fitting functions obtained by linear regression analyses (see the text for details).

annihilation process at the molecular orbital level.^{40,41} These studies presented that the inner valence shell (the lowest occupied orbital) electrons may possess especially dominant contributions to the annihilation. In contrast, the conventional linear fitting¹⁶ can be obtained explicitly to contain the number of π -electrons as an explanatory variable, and the case study for the positron annihilation rate of fluorinated benzenes³¹ also showed the obvious result that the largest contributions to the two-photon annihilation rate arose from the valence 2p-derived orbitals including π -like orbitals but not from the lowest 2p-derived orbitals. Thus, the molecular level mechanism of the positron annihilation is still controversial. From this perspective, biological molecular systems also become an important model to test the above theoretical aspects.

In the present study, we investigated positron binding and annihilation properties systematically for the global minimum (GM) and the hydrogen-bonded (HB) conformers for each of the 20 standard amino acids: Ala, Arg, Asn, Asp, Cys, Gln, Glu, Gly, His, Ile, Leu, Lys, Met, Phe, Pro, Ser, Thr, Trp, Tyr, and Val, using the MC_MO-based HF method. The GM and HB structures of the amino acids have quite distinct properties due to geometries of a carboxy hydrogen atom, which significantly affect these positron binding abilities: the HB structures have larger dipole moments than the GM structures and are several tens of millielectron volts higher in energy relative to the GM structures. Although these amino acid molecules are mostly known to have about 8–10 eV of the ionization energy^{42,43} as large as in the case of large alkane species mentioned above, some of these amino acids, particularly, most of the HB structures can form stable positronic bound states due to such large dipole moments but independent of the ionization energy (see Figure S1). As for calculations of annihilation rates, we applied the enhancement factor^{44–46} (see the Computational Details section) for improving the low qualities of the HF level calculation results. By utilizing one-particle properties for the electron–positron contact density obtained by the present MC_MO-based HF calculations, we analyzed the positron

annihilation properties related to both characteristics of electronic and positronic structures.

RESULTS AND DISCUSSION

Positron Affinity and Annihilation Rate. First, we calculated the positron affinity PA and the two-photon annihilation rate Γ_2^{HF} using the MC_MO HF method with the 6-311+G(3d,3p) electronic and two-atom-center situated [9s9p] positronic basis sets, and Γ_2^{γ} including corrections by the enhancement factor for both GM and HB structures of all amino acid molecules (see the Computational Details section for details). Table 1 shows the calculation results for GM and HB amino acids predicted to have positive PAs (i.e., capable of binding to a positron) by the present MC_MO HF and the earlier APMO HF and APMO P2 calculations by Charry et al.³⁸ for comparisons. All detailed numerical data obtained in this work are available in Table S3. The results showed that all of the HB structures exhibit positive PAs, while for the GM structures, only three amino acid species, Gln-GM, His-GM, and Trp-GM, can have positive PAs at the HF level. In comparison with the latest calculation results for PA at the HF level (APMO HF) reported by Charry et al.,³⁸ the present calculations using the two-atom-center positronic basis set give $\sim 10\%$ smaller PAs only for some HB species, such as Ala-HB, Arg-HB, Glu-HB, Pro-HB, Trp-HB, and Val-HB, regarded as the strongly polar HB species having dipole moments greater than ~ 5.5 debye, while these give larger PAs particularly for all three GM species and some HB species, such as His-HB, Ser-HB, and Thr-HB with comparatively small dipole moments rather.

For amino acid species shown in Table 1, we show PA (in meV) as a function of the dipole moment μ (in debye) of the parent amino acids in Figure 1a, where the solid line indicates a fitting function obtained by the linear regression analysis for PA with respect to μ . In this linear regression, the fitted line $\text{PA}(\mu) = 22.218\mu - 79.568$ shows the correlation coefficient $R^2 = 0.931$, which roughly agrees with the previous calculation results at the HF level.^{34,38} The obtained critical dipole moment $\mu_c = 3.581$ debye is larger than Crawford's critical value $\mu = 1.625$.⁴⁷ By

inclusion of the electron–positron correlation effect with the APMO-based many-body theoretical calculations³⁸ (e.g., APMO P2 calculations shown in Table 1), PAs by HF level calculations increase by ~50% or more, and a positronic system (e.g., [Ser; e⁺]) predicted to be unstable by the HF level calculations is inverted to be stable, as shown in Table 1. Consequently, it was found that due to such significant correlation effects, the critical dipole moment μ_c decreases from expectations of the HF calculation results, and the linearity of PA with respect to μ is somewhat weakened for increased PAs.³⁸ However, the important trend that PA increases depending dominantly on μ of the parent molecule can be maintained.

In the qualitative aspects of HF level calculation results, we found a disagreement result only for the [Trp-GM; e⁺] with the previous studies. The present and Koyanagi et al.³⁴ commonly predicted positive PAs as 2.44 and 4.0 meV, respectively, while Charry et al.³⁸ presented a negative PA (i.e., no positron binding ability) even in MP2 and P2 calculations. This discrepancy for the [Trp-GM; e⁺] system arises from the difference in the optimized equilibrium geometries that show different dipole moments: our work and Koyanagi et al. showed $\mu = 4.1$ and 4.0 debye, respectively, while Charry et al. showed $\mu = 1.19$ debye, for the parent Trp system. Referring to the other detailed study for conformations of Trp,⁴⁸ the GM structure in this work can be considered as the most stable structure showing $\mu = 3.99$ debye, while the other one may be identified as one of the lowest energy conformers lying slightly higher in energy, showing $\mu = 1.18$ debye with a different scheme of hydrogen bonding. However, even more importantly, these results suggest that the positron binding ability is sensitive to the conformational geometry.

For the positron annihilation property, since the annihilation rate is known to be proportional to the parameter,^{16,49} we examined the linear dependence on $\sqrt{\text{PA}}$ for both data sets, Γ_2^{HF} (black circles) obtained by eq 6 at the HF level and Γ_2^{γ} (red triangles) including corrections by the enhancement factor, as represented in Figure 1b, where both Γ_2^{HF} and Γ_2^{γ} are shown in units of ns⁻¹. We found that due to the enhancement factor, annihilation rates for HB structures increased by a factor of ~4.0, while those for the GM structures increased by factors of 4.2–4.6, compared to values at the HF level. These trends on the effects of the enhancement factor are similar to the case of alkane molecules.⁴⁶ For the present amino acids, the fitted functions obtained by the regression analyses with respect to $\sqrt{\text{PA}}$, $\Gamma_2^{\text{HF}} = 0.00245\sqrt{\text{PA}} - 0.00328$ and $\Gamma_2^{\gamma} = 0.00948\sqrt{\text{PA}} - 0.0118$, show correlation coefficients $R^2 = 0.964$ and 0.962 , respectively, which indicate that a linear relation between the annihilation rate and the square root of the positron affinity holds for the amino acid molecules. However, the fitted functions for both Γ_2^{HF} and Γ_2^{γ} have unfavorably finite (nonzero) intercepts giving critical PA values, $\text{PA}_c = 1.79$ and 1.55 meV, respectively. This might be attributed to the insufficient accuracy for interparticle correlations in the mean-field HF approximation that is difficult to reproduce the positron binding energy qualitatively, particularly for loosely bound positrons of weak polar systems, or to slower convergence of the electron–positron contact density in comparison with the positron affinity in the variational method.

In the particular cases of [Gln-GM; e⁺], [His-GM; e⁺], and [Trp-GM; e⁺] systems mentioned above, we also obtained that the use of the present two-atom-center positronic basis set effectively enhanced Γ_2^{HF} compared to the use of a similar size of

the one-atom-center positronic basis set even in the HF approximation (see Table S2). This effect is expected to be associated with delocalization characteristics of positronic wave functions for the loosely bound positrons, particularly for such GM structures.

Positronic Structure. Figure 2 shows the positronic wave functions (the singly occupied positron orbitals) for a simple HB

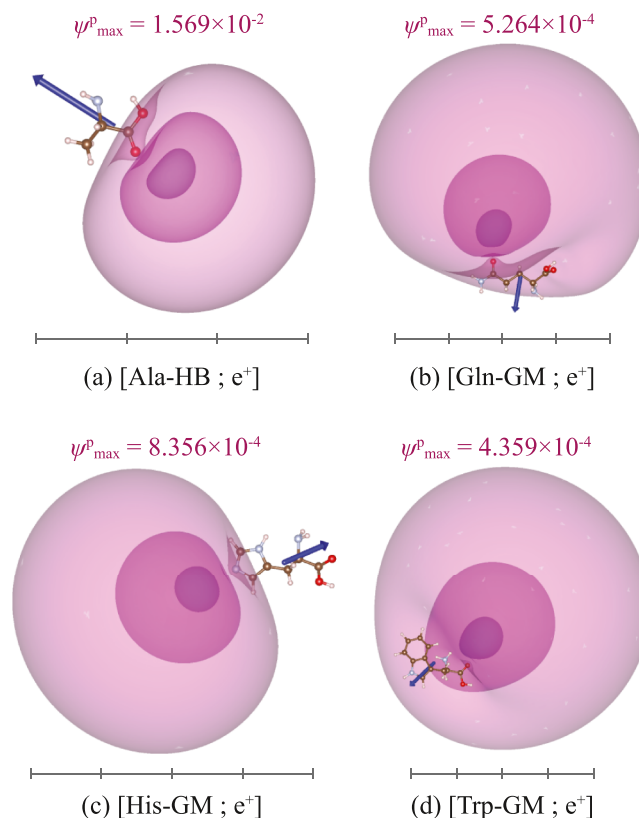


Figure 2. Positron orbitals for (a) [Ala-HB; e⁺], (b) [Gln-GM; e⁺], (c) [His-GM; e⁺], and (d) [Trp-GM; e⁺] systems, where pink-to-purple surfaces show positronic wave function isosurfaces in a.u., and embedded blue arrows show electric dipole moment vectors. Isosurfaces with 90, 60, and 30% of the maximum value ψ_{max}^p are enclosed from the inner (purple) to the outer (thin pink). Hydrogen, carbon, nitrogen, and oxygen atoms are indicated by white, brown, gray, and red balls, respectively. Horizontal ticks below the positronic wave functions are shown for every 5 Å.

system [Ala-HB; e⁺] as a representative system of the HB structures, and for three GM systems, [Gln-GM; e⁺], [His-GM; e⁺], and [Trp-GM; e⁺], which are expected to have comparatively delocalized positronic orbitals. These positronic orbital maxima ψ_{max}^p can be found to align with the dipole moment vectors of parent molecules, indicated by blue arrows, which are associated with distributions of the (local) negative electrostatic potentials. Such situations can be, in general, obtained in the vicinity of an oxygen atom with a lone pair in a carboxy group for both [Ala-HB; e⁺] and [Trp-GM; e⁺] systems as well as all cases of the other HB structures (see Figure S3). In this situation, a lone pair in the carboxy oxygen atom can be considered to play a role in inducing the electric field to attract a positron. On the other hand, different situations for ψ_{max}^p can be found only in [Gln-GM; e⁺] and [His-GM; e⁺], where ψ_{max}^p is located in the vicinity of a side-chain oxygen atom for [Gln-GM; e⁺] and that of a nitrogen atom in a side-chain five-membered

ring for [His-GM; e⁺]. For these GM species, a hydrogen atom in a terminal carboxy group forms a hydrogen bond with a neighboring oxygen atom with a lone pair. This hydrogen bonding reduces the negative electrostatic potential around the carboxy oxygen atom, while the remaining active lone pair electrons in the side chain dominantly contribute to the molecular gross dipole moment favored in binding a positron. The capability of binding a positron by a terminal nitrogen contributing to the gross dipole moment with a lone pair in the organic molecule was reported in the case study for the positronic nitrile species.²²

For more details, in cases of the GM structures, particularly, [Gln-GM; e⁺] and [Trp-GM; e⁺] shown in Figure 2b,d, respectively, the positronic orbitals can be found to be fairly delocalized from locations of the orbital maxima to vicinities of other atomic nuclei concerned with lone pair electrons. For these loosely bound positrons, the positronic orbital maxima $\psi_{\max}^p \sim 10^{-4}$ au are smaller in comparison to $\psi_{\max}^p \sim 10^{-3}$ – 10^{-2} au for cases of the HB structures as represented by [Ala-HB; e⁺] having comparatively localized positronic orbitals. For [Gln-GM; e⁺], the positronic orbital extends from the vicinity of an oxygen atom in a side chain to near oxygen atoms constituting a carboxy group. For [Trp-GM; e⁺], the positronic orbital extends to around the amino group nitrogen atom with a lone pair as well as the six-membered ring of a side chain. These delocalization behaviors of the bound positrons are also due to the electronic structure causing partial polarization supporting to bind a positron.

Importantly, the strongly delocalized features of the positronic orbitals suggest that it is also probable that the annihilation of an attached positron occurs due to contact with either electrons coming from functional groups related to delocalized electronic orbitals. Toward understanding this issue, we will discuss the details about the electron–positron contact density $\langle \delta_{ep} \rangle$ in the following section.

Analysis of the Electron–Positron Pair Annihilation.

To figure out properties of the electron–positron pair annihilation rates for the positronic amino acid compounds, we analyzed the quantity $\rho^{\text{ep}}(r)$ in eq 4 representing the probability density that electrons and a positron are found in the same position and decomposition of the electron–positron pair annihilation rates into the components Γ_2^i by eq 6. The $\rho^{\text{ep}}(r)$ distribution gives us more practical information about the electron–positron contact causing the occurrence of positron annihilation rather than individual electronic and positronic molecular orbitals as seen above. Figure 3 shows $\rho_{ep}(r)$ for [Ala-HB; e⁺], [Trp-GM; e⁺], [His-GM; e⁺], and [Gln-GM; e⁺], of which the positronic structures have been dealt with in the discussion in the above section. For the [Ala-HB; e⁺] system, the contact density maxima ρ_{\max}^{ep} can be clearly found in the vicinity of both oxygen atoms constituting a carboxy group. Similarly, ρ_{\max}^{ep} for cases of the GM structures of [Trp-GM; e⁺], [His-GM; e⁺], and [Gln-GM; e⁺] can be found to appear at almost the same locations to ψ_{\max}^p (c.f. Figure 2). However, non-negligible density local maxima as showing at least 5–30% of ρ_{\max}^{ep} can be found at a terminal carboxy group for [Gln-GM; e⁺] and at around both sides of an amino group and a six-membered ring for [Trp-GM; e⁺]. In the [His-GM; e⁺] case, such ρ^{ep} local maxima can be found only around hydrogen atoms neighboring a nitrogen atom with a lone pair in a five-membered ring. The delocalization of the positronic wave function significantly affects the extent of delocalized $\rho^{\text{ep}}(r)$ distributions as postulated above.

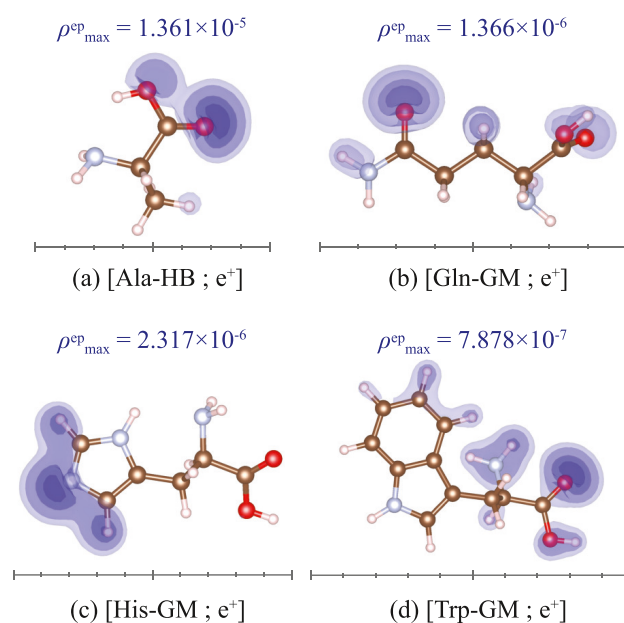


Figure 3. Collision probability densities $\rho^{\text{ep}}(r)$ calculated by the MC_MO HF method for (a) [Ala-HB; e⁺], (b) [Gln-GM; e⁺], (c) [His-GM; e⁺], and (d) [Trp-GM; e⁺] systems. Dark blue surfaces show density isosurfaces with 60, 30%, 10, and 5% of the maximum value ρ_{\max}^{ep} enclosed from the inner to the outer, in units of au. Hydrogen, carbon, nitrogen, and oxygen atoms are indicated by white, brown, gray, and red balls, respectively. Horizontal ticks below the contact densities are shown for every 1 Å.

More details of the annihilation properties can be obtained by decomposition of the annihilation rates into the components Γ_2^i for one-electron orbitals ψ_i^e . In Figure 4, Γ_2^i spectra with respect to the electronic molecular orbital energy ε_i lying above -1.6 Hartree are represented by histograms with thin blue and orange bars for both Γ_2^{HF} at the HF level (the left panels) and Γ_2^{enh} including corrections with the enhancement factor (the right panel) for (a) [Ala-HB; e⁺], (b) [Gln-GM; e⁺], (c) [His-GM; e⁺], and (d) [Trp-GM; e⁺] systems. The electronic orbital energies involve all electronic molecular orbitals derived from the valence shells for these systems, which contribute to the electron–positron pair annihilation rate accounting for the majority (at least 95%) of the total annihilation rates. In this analysis, although the order of electronic orbital energies is approximated by the HF approximation, it can be shown that some certain local peaks appear at electronic orbitals lying near HOMO (above approximately $\varepsilon_i = -0.6$ Hartree) and even deeper energy levels, as illustrated by orange bars with orbital insets labeled by P_i ($i = 1$ – 4). For [Ala-HB; e⁺], the uppermost peak P_1 and the second one P_2 are characterized as the O–C–O antibonding $2p\pi$ -like (out-of-plane) orbital and the C–O bonding $2p\sigma$ -like (in-plane) orbital with respect to a carboxy COO plane, respectively (here, the bond notation X–Y means an interatomic connection between atoms X and Y but does not mean the bond order). These P_1 and P_2 peaks are maintained in the decomposition of Γ_2^{enh} due to the effects of the enhancement factor that effectively affects energetically higher occupied orbitals. The positronic wave function overlaps with not only the σ -type but also the π -type bonding electrons of a lone pair can be considered to contribute to the $\rho^{\text{ep}}(r)$ maxima found in [Ala-HB; e⁺]. P_3 and P_4 lying below $\varepsilon_i = -1.4$ Hartree are characterized as C–O σ -like orbitals dominantly contributed from the C 2s and O 2s electrons of a carboxy. However,

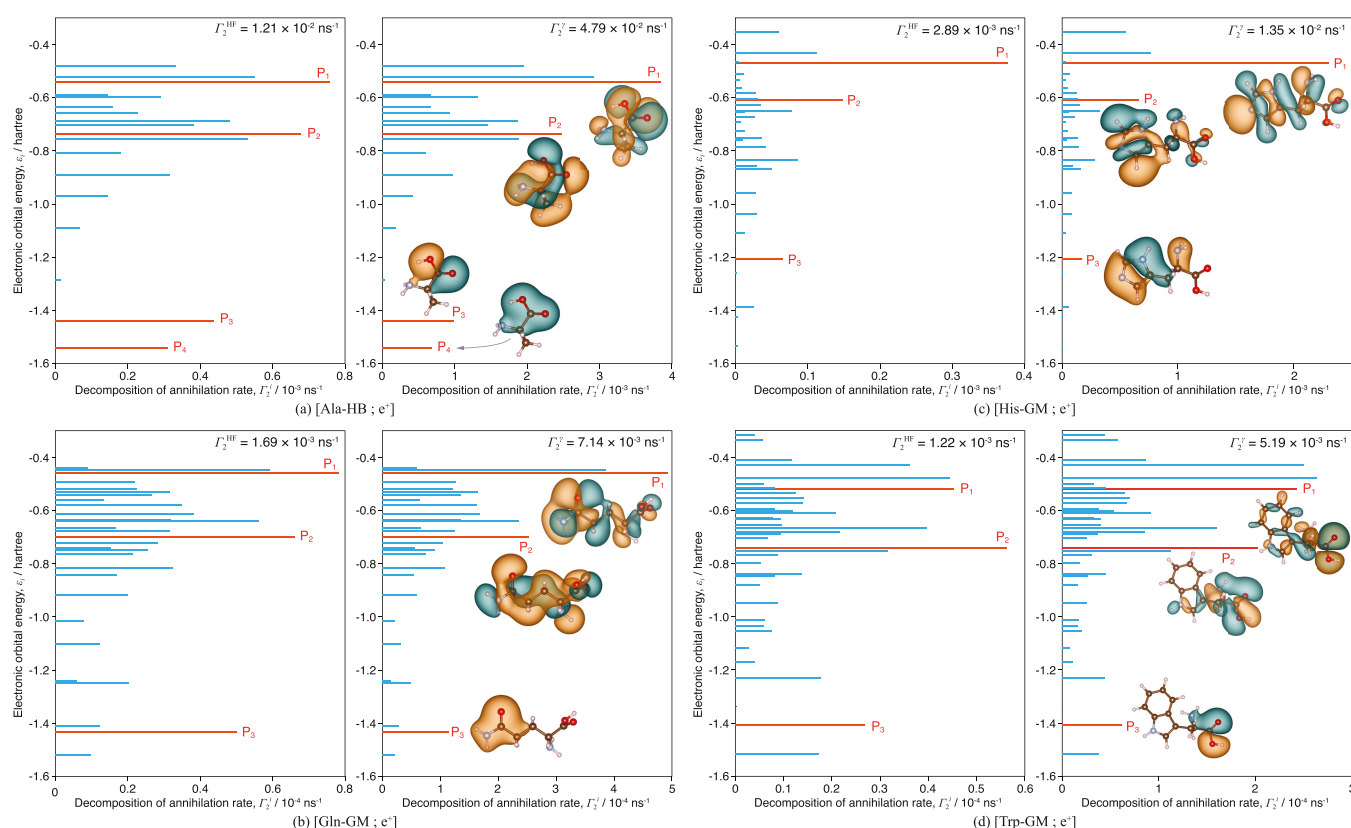


Figure 4. Decomposition of two-photon annihilation rates, Γ_2^{HF} (left panels) and Γ_2^i (right panels), into the components for electronic molecular orbitals for (a) [Ala-HB; e^+], (b) [Gln-GM; e^+], (c) [His-GM; e^+], and (d) [Trp-GM; e^+] systems. The vertical and the horizontal axes show the electronic orbital energy ε_i and the component Γ_2^i obtained by the MC_MO HF calculations. Γ_2^i for both Γ_2^{HF} and Γ_2^i are shown as a spectrum-like representation with blue and orange lines. Inset figures show the electronic molecular orbitals picked up (see the text), indicated by orange lines, where brown and green wave function isosurfaces correspond to ± 0.1 au, respectively.

contributions from these inner valence shells become comparatively smaller due to corrections by the enhancement factor. These trends can be found in most cases of the other HB structures (see Figure S4).

In the [Gln-GM; e^+] system shown in Figure 4b, for which the positron orbital maxima ψ_p^{max} is located near an oxygen having a lone pair in a side chain (Figure 2b), three Γ_2^i peaks assigned as P_1 , P_2 , and P_3 also appear from the nonbonding type inplane O 2p orbital, the C–O bonding $2p\sigma$ -like orbital, and the C–O bonding $2s\sigma$ -like orbital, with respect to the side chain CNO plane, respectively. In the [His-GM; e^+] system shown in Figure 4c, where the positron is bound to a nitrogen atom with a lone pair, obviously, Γ_2^i peaks assigned as P_1 , P_2 , and P_3 appear from electronic orbitals for N–H and C–H inplane orbitals. For these two GM species (b) and (c), the upper two peaks P_1 and P_2 are even greater due to the effect of the enhancement factor, while the contribution from P_3 of the inner valence orbitals becomes relatively small. In the [Trp-GM; e^+] system, two Γ_2^i peaks, P_2 and P_3 appear from the electronic orbitals contributing to the formation of the NH–HO bonding between an amino and a carboxy group neighboring to each other. The electronic orbitals yielding the uppermost peak P_1 have somewhat delocalized characteristics as extending to a six-membered ring of a side chain. The local maxima of $\rho^{\text{ep}}(r)$ are deeply connected to such delocalized electronic orbitals to increase the wave function overlap with the delocalized positronic orbital. Furthermore, due to corrections with the enhancement factor, contributions from this delocalized electronic orbital and higher energy valence orbitals increase significantly.

By analyses of the one-particle property for the annihilation rates, we clarified that the greater part of $\rho^{\text{ep}}(r)$ is led by the positronic wave function overlap with both σ - and π -type lone pair electrons to induce the local electrostatic potential. A similar mechanism for Γ_2 was found in the case study for the positron annihilation on fluorinated benzene,³¹ whereas the present systems showed that delocalization characteristics of both electrons and a positron have the crucial role to enhance $\rho^{\text{ep}}(r)$ as quantified by the Γ_2^i peaks. The present analytical results are quite in disagreement with the claim^{40,41} that s-type inner valence shell electrons yield a significant contribution to positron annihilation. However, such simplification may be qualified for simple systems of highly symmetric electronic structures but is not valid for complicated organic molecules represented by biological molecules possessing functional groups at least. A more complicated mechanism for positron annihilation may also be postulated for other molecular compounds and clusters formed by various chemical bonding schemes.

In addition, employing the multi-atom-center situated positronic basis functions were effective for increasing the electron–positron pair annihilation rate related to both loosely bound positronic and dominant electronic orbitals even at the HF level, particularly for the large sizes of amino acids with comparatively small dipole moment magnitudes, such as [Gln-GM; e^+] and [Trp-GM; e^+]. As for these species, Γ_2^i components correspond to all assigned local peaks p_i increased by ~ 2 times compared to the use of a similar number of the one-atom-center positronic basis functions (c.f. the same analytical result for Γ_2

calculated using one-atom-center positronic basis functions as shown in Figure S5). In utilizing the one-particle properties obtained by the HF level calculations for corrections via the enhancement factor, the use of multicenter situated basis functions for the positron may be one of the useful ways to obtain enhanced electron–positron contact densities within the independent-particle theoretical framework. The present results can be further improved using appropriate multicenter positronic basis functions with large expansions, which was necessary for localized features of strongly bound positrons particularly for most of the HB structures, as shown in the previous report by Charry et al.³⁸

CONCLUSIONS

We investigated the positron binding and positron annihilation properties for the global minimum and the hydrogen-bonded structures for 20 amino acid molecules using the multicomponent molecular orbital method. Applying two-atom-center situated positronic basis functions for expressions of loosely bound positrons was effective for minimizing the total energy of the positronic amino acid compounds (i.e., maximizing the positron affinity) and for reproducing enhancements of the electron–positron contact densities, particularly for weakly bound positronic systems. To improve the low accuracy of the multicomponent Hartree–Fock level calculations for the two-photon annihilation rates, we also applied corrections by the enhancement factor to one-particle properties of annihilation rates. Our regression analysis showed that the positron affinity can be characterized simply by the molecular electrostatic properties as the permanent dipole moment, and the linear dependence of the two-photon annihilation rates on the square root of the positron affinity holds for the amino acids. Furthermore, by the one-particle property analysis for the annihilation rate, we found that delocalization characteristics of both electrons and a positron play a key role in enhancing the positron annihilation rate arising from both the valence electrons in σ - and π -type molecular orbitals from 2p atomic orbitals but not from the highest occupied molecular orbital electrons, especially for the global minimum structures with loosely bound positrons. These components of the annihilation rates yield greater contributions due to the effect of the enhancement factor. For more accurate results, higher-level first-principles calculations involving interparticle correlation effects are needed for resolving stabilities of the positronic bound states particularly for weakly polar amino acid species, e.g., most of the GM structures, where the effect of the partial polarizability may be crucial for positron binding. These issues are to be addressed in our future work.

COMPUTATIONAL DETAILS

Total energies for the positronic compounds are calculated using the multicomponent molecular orbital (MC_MO) method. In the MC_MO theoretical framework, the multicomponent wave function containing the electronic Slater determinant and the positronic orbital can be obtained by solving the electronic and the positronic Roothaan equations, simultaneously (see refs 50, 51 for the details). In this work, we calculated the total energies $E[X]$ for the system X of the amino acid molecule at the equilibrium nuclear geometry, and $E[X; e^+]$ for the same system containing a positron, $[X; e^+]$ using the Hartree–Fock (HF) level of the MC_MO theory. As shown in previous studies for the positronic amino acid species,^{34–36} the

positrons are loosely bound to the systems and nuclear relaxation due to the positron attachment to systems may be considered negligible. Therefore, we define the positron affinity (PA) for the system X as

$$PA = E[X] - E[X; e^+] \quad (1)$$

Since the positronic amino acids have closed electronic shell subsystems, we will calculate the electron–positron annihilation rate for the two-photon process, Γ_2 , described by

$$\Gamma_2 = \pi\alpha^4 a_0^2 c \langle \delta_{ep} \rangle \quad (2)$$

where α , a_0 , and c are the fine structure constant, the classical Bohr radius, and the light velocity in a vacuum, respectively, and $\langle \delta_{ep} \rangle$ is the electron–positron contact density representing the number of the electron–positron coalescence per unit volume. In the MC_MO framework, using the i -th doubly occupied electronic orbital $\psi_i^e(\mathbf{r})$ and the singly occupied positronic orbital $\psi_i^p(\mathbf{r})$ for the positronic molecular system containing N_e electrons, $\langle \delta_{ep} \rangle$ can be represented in terms of the electron–positron collision probability density $\rho^{ep}(\mathbf{r}_p)$

$$\langle \delta_{ep} \rangle = \int \rho^{ep}(\mathbf{r}_p) d\mathbf{r}_p \quad (3)$$

and

$$\rho^{ep}(\mathbf{r}) = \sum_{i=1}^{N_e/2} n_i \psi_i^e(\mathbf{r}) \psi_i^e(\mathbf{r}) \psi_i^p(\mathbf{r}) \psi_i^p(\mathbf{r}) \quad (4)$$

where $n_i = 2$ for closed-shell electronic systems. Thus, the electron–positron contact density $\rho^{ep}(\mathbf{r}_p)$ can be evaluated simply by the multiplication of the total electron density $2 \sum_{i=1}^{N_e/2} |\psi_i^e(\mathbf{r})|^2$ by the positron density $|\psi^p(\mathbf{r})|^2$. In addition, by decomposing the annihilation rate Γ_2^{HF} calculated by the MC_MO HF method in eq 2 into components Γ_2^i for electronic molecular orbitals as

$$\Gamma_2^{\text{HF}} = 2 \sum_{i=1}^{N_e/2} \Gamma_2^i \quad (5)$$

where

$$\Gamma_2^i = \pi\alpha^4 a_0^2 c \int \psi_i^e(\mathbf{r}) \psi_i^e(\mathbf{r}) \psi_i^p(\mathbf{r}) \psi_i^p(\mathbf{r}) d\mathbf{r} \quad (6)$$

we can obtain the two-photon annihilation rate obtained by the probability of the collision between an electron occupying the i -th electronic orbital and a positron. In addition, the electron–positron contact density calculated via the independent-particle approximation was corrected by the enhancement factor, which was developed by Green and Gribakin⁴⁴ using the many-body perturbation theory to take into account the electron–positron annihilation vertex corrections. An empirical formula for the electronic orbital-specific enhancement factor introduced by Green and Gribakin⁴⁴ is written by

$$\gamma_i = 1 + \sqrt{\frac{1.31}{-\varepsilon_i}} + \left(\frac{0.834}{-\varepsilon_i} \right)^{2.15} \quad (7)$$

where i is an electronic orbital number and ε_i (<0) is the i -th occupied electronic orbital energy. Using this factor, eq 5 is corrected as

$$\Gamma_2^\gamma = 2 \sum_{i=1}^{N_e/2} \gamma_i \Gamma_2^i \quad (8)$$

The present system of the amino acid X contains both the global minimum and the hydrogen-bonded structures for 20 standard amino acids: Ala, Arg, Asn, Asp, Cys, Gln, Glu, Gly, His, Ile, Leu, Lys, Met, Phe, Pro, Ser, Thr, Trp, Tyr, and Val. We used the Pople type triple-zeta split valence basis set, 6-311+G(3d, 3p), including the diffuse functions for the second-row species and three d-type and three p-type polarization functions for the first- and the second-row species, respectively, for the electron, and the two-atom-center situated Gaussian type [9s9p] basis functions for the positron (i.e., in total [18s18p] basis functions are employed). Different two basis function centers were appropriately selected to obtain the lowest total energies for positronic compounds, considering partial negative electrostatic potential maps: two oxygen atoms in a carboxy group for HB structures, an oxygen atom of a side chain, and a lone pair oxygen atom of a carboxy group for Gln-GM, a lone pair nitrogen atom of a side chain and a lone pair oxygen atom of a carboxy group for Trp-GM, and a nitrogen atom of an amino group and a lone pair oxygen atom of a carboxy group for His-GM (see Table S2 for test calculations). The Gaussian exponents are determined in the even-tempered scheme as $\alpha_{i+1} = c \times \alpha_i$ with $c = \sqrt{10}$ and $\alpha_1 = \sqrt{10} \times 10^{-4}$ and 10^{-4} for the s- and p-type functions, respectively, for each of the different atom-center [9s9p] sets. In this work, all of the calculations were performed using our MC_MO modified version of the GAMESS package.^{52,53} The four-center overlap integrals in eq 6 were calculated using the Obara–Saika scheme⁵⁴ implemented in the modified GAMESS.

As proposed by Tachikawa et al. in their fully variational molecular orbital studies,^{51,55} ideally, basis function centers and exponents should also be variationally optimized to obtain the best wave function in the MC_MO theoretical framework. There are some theoretical performances using such floating Gaussian function methods for positronic small molecular systems.^{23,56} However, it would be difficult in practice to fulfill the fully variational optimization of the basis sets particularly for large polyatomic systems as the present. For these reasons, previous studies on positronic amino acids have attempted to approximate the wave function of a bound positron by an appropriate choice of the single orbital center,^{34,38} under reasonable criteria, e.g., minimizing the total energies for positronic compounds. In comparison with the use of the positronic one-atom-center basis set including more nodal functions as d and f types, the two-atom-center basis set employed in this work can reproduce the consistent results for PA and can simultaneously increase Γ_2 (see Table S2). Increasing Γ_2 via such a multi-atom-center positronic basis set reflects the nature of positron annihilation for a loosely bound positron, as discussed in this paper in detail.

■ ASSOCIATED CONTENT

Supporting Information

The Supporting Information is available free of charge at <https://pubs.acs.org/doi/10.1021/acsomega.1c03409>.

Experimental ionization energies for amino acids (Table S1); the positron affinity (PA) as a function of the electronic highest occupied molecular orbital energy for the present amino acids, obtained in this work (Figure S1), illustration of electrostatic potentials of the amino acids to be concerned with the choice of positronic basis function centers in this work (Figure S2); test calculations which present the dependence of PA on the positronic basis function center (Table S2); numerical details of the

present calculation results (Table S3); positron orbitals for [X; e⁺] for all amino acids X having positive PAs (Figure S3); and electron–positron collision probability densities and decomposition of two-photon annihilation rates calculated using two-atom-center and one-atom-center positronic basis functions for [X; e⁺] for all amino acids X having positive PAs (Figures S4 and S5) (PDF)

■ AUTHOR INFORMATION

Corresponding Authors

Maya Ozaki – Quantum Chemistry Division, Yokohama City University, Yokohama 236-0027, Japan; Email: n195209a@yokohama-cu.ac.jp

Daisuke Yoshida – Quantum Chemistry Division, Yokohama City University, Yokohama 236-0027, Japan;  orcid.org/0000-0002-5843-2629; Email: daiy@yokohama-cu.ac.jp

Yukiumi Kita – Quantum Chemistry Division, Yokohama City University, Yokohama 236-0027, Japan; Email: ykita@yokohama-cu.ac.jp

Tomomi Shimazaki – Quantum Chemistry Division, Yokohama City University, Yokohama 236-0027, Japan; Email: tshima@yokohama-cu.ac.jp

Masanori Tachikawa – Quantum Chemistry Division, Yokohama City University, Yokohama 236-0027, Japan;  orcid.org/0000-0002-5489-5714; Email: tachi@yokohama-cu.ac.jp

Complete contact information is available at: <https://pubs.acs.org/10.1021/acsomega.1c03409>

Notes

The authors declare no competing financial interest.

■ ACKNOWLEDGMENTS

This work was partly supported by Grants-in-Aid for Scientific Research (KAKENHI) of the Ministry of Education, Culture, Sports, Science and Technology (MEXT) (Grant Nos. 18H01945, 19H05063, and 19H05155 for M.T. and Grant No. 18K05041 for Y.K.). The computations were partly performed using the resources provided by the Research Center for Computational Science (RCCS), Okazaki, Japan.

■ REFERENCES

- (1) Tuomisto, F.; Makkonen, I. Defect identification in semiconductors with positron annihilation: Experiment and theory. *Rev. Mod. Phys.* **2013**, *85*, 1583–1631.
- (2) Shon, I. H.; O'Doherty, M. J.; Maisey, M. N. Positron emission tomography in lung cancer. *Semin. Nucl. Med.* **2002**, *32*, 240–271.
- (3) Wahl, R. L.; Siegel, B. A.; Edward Coleman, R.; Gatsonis, C. G. Prospective multicenter study of axillary nodal staging by positron emission tomography in breast cancer: a report of the staging breast cancer with PET study group. *J. Clin. Oncol.* **2004**, *22*, 277–285.
- (4) Reivich, M.; Kuhl, D.; Wolf, A.; Greenberg, J.; Phelps, M.; Ido, T.; Casella, V.; Fowler, J.; Hoffman, E.; Alavi, A.; Som, P.; Sokoloff, L. The [¹⁸F]fluorodeoxyglucose method for the measurement of local cerebral glucose utilization in man. *Circ. Res.* **1979**, *44*, 127–137.
- (5) Ryzhikh, G. G.; Mitroy, J.; Varga, K. The structure of exotic atoms containing positrons and positronium. *J. Phys. B* **1998**, *31*, 3965–3996.
- (6) Ryzhikh, G. G.; Mitroy, J. Positron annihilation profiles for HPs and He(³S^e)e⁺. *J. Phys. B* **1999**, *32*, 4051–4064.
- (7) Mitroy, J.; Ryzhikh, G. G. Improved binding energies for LiPs, e⁺Be, NaPs and e⁺Mg. *J. Phys. B* **2001**, *34*, 2001–2007.
- (8) Swalina, C.; Pak, M. V.; Hammes-Schiffer, S. Analysis of electron-positron wavefunctions in the nuclear-electronic orbital framework. *J. Chem. Phys.* **2012**, *136*, No. 164105.

- (9) Gilbert, S. J.; Greaves, R. G.; Surko, C. M. Positron scattering from atoms and molecules at low energies. *Phys. Rev. Lett.* **1999**, *82*, 5032–5035.
- (10) Barnes, L. D.; Gilbert, S. J.; Surko, C. M. Energy-resolved positron annihilation for molecules. *Phys. Rev. A* **2003**, *67*, No. 032706.
- (11) Barnes, L. D.; A, Y. J.; Surko, C. M. Energy-resolved positron annihilation rates for molecules. *Phys. Rev. A* **2006**, *74*, No. 012706.
- (12) Young, J. A.; Surko, C. M. Positron attachment to molecules. *Phys. Status Solidi C* **2009**, *6*, 2265–2271.
- (13) Danielson, J. R.; Young, J. A.; Surko, C. M. Dependence of positron-molecule binding energies on molecular properties. *J. Phys. B* **2009**, *42*, No. 235203.
- (14) Jones, A. C. L.; Danielson, J. R.; Gosselin, J. J.; Natisin, M. R.; Surko, C. M. Positron binding to alcohol molecules. *New J. Phys.* **2012**, *14*, No. 015006.
- (15) Mitroy, J.; Bromley, M. W. J.; Ryzhikh, G. G. Positron binding to a model alkali atom. *J. Phys. B* **1999**, *32*, 2203–2214.
- (16) Gribakin, G. F.; Young, J. A.; Surko, C. M. Positron-molecule interactions: Resonant attachment, annihilation, and bound states. *Rev. Mod. Phys.* **2010**, *82*, 2557–2607.
- (17) Strasburger, K. Quantum chemical study on complexes of the LiH molecule with e^+ , Ps and Ps^- including correlation energy. *Chem. Phys. Lett.* **1996**, *253*, 49–52.
- (18) Tachikawa, M.; Buenker, R. J.; Kimura, M. Bound states of positron with urea and acetone molecules using configuration interaction *ab initio* molecular orbital approach. *J. Chem. Phys.* **2003**, *119*, 5005.
- (19) Strasburger, K. Positronic formaldehyde—the configuration interaction study. *Struct. Chem.* **2004**, *15*, 415–420.
- (20) Buenker, R. J.; Liebermann, H.; Melnikov, V.; Tachikawa, M.; Pichl, L.; Kimura, M. Positron binding energies for alkali hydrides. *J. Phys. Chem. A* **2005**, *109*, 5956–5964.
- (21) Chojnacki, H.; Strasburger, K. Configuration interaction study of the positronic hydrogen cyanide molecule. *Mol. Phys.* **2006**, *104*, 2273–2276.
- (22) Tachikawa, M.; Kita, Y.; Buenker, R. J. Bound states of the positron with nitrile species with a configuration interaction multi-component molecular orbital approach. *Phys. Chem. Chem. Phys.* **2011**, *13*, 2701–2705.
- (23) Oyamada, T.; Tachikawa, M. Multi-component molecular orbital study on positron attachment to alkali-metal hydride molecules: nature of chemical bonding and dissociation limits of $[LiH;e^+]$. *Eur. Phys. J. D* **2014**, *68*, No. 231.
- (24) Mella, M.; Morosi, G.; Bressanini, D.; Elli, S. Positron and positronium chemistry by quantum Monte Carlo. V. The ground state potential energy curve of e^+LiH . *J. Chem. Phys.* **2000**, *113*, 6154.
- (25) Kita, Y.; Maezono, R.; Tachikawa, M.; Towler, M.; Needs, R. J. *Ab initio* quantum Monte Carlo study of the positronic hydrogen cyanide molecule. *J. Chem. Phys.* **2009**, *131*, No. 134310.
- (26) Kita, Y.; Maezono, R.; Tachikawa, M.; Towler, M. D.; Needs, R. J. *Ab initio* quantum Monte Carlo study of the binding of a positron to alkali-metal hydrides. *J. Chem. Phys.* **2011**, *135*, No. 054108.
- (27) Mitroy, J.; Bubin, S.; Horiuchi, W.; Suzuki, Y.; Adamowicz, L.; Cencek, W.; Szalewicz, K.; Komasa, J.; Blume, D.; Varga, K. Theory and application of explicitly correlated Gaussians. *Rev. Mod. Phys.* **2013**, *85*, 693–749.
- (28) Sugiura, Y.; Suzuki, H.; Otomo, T.; Miyazaki, T.; Takayanagi, T.; Tachikawa, M. Positron-electron correlation-polarization potential model for positron binding in polyatomic molecules. *J. Comput. Chem.* **2020**, *41*, 1576–1585.
- (29) Swann, A. R.; Gribakin, G. F. Effect of molecular constitution and conformation on positron binding and annihilation in alkanes. *J. Chem. Phys.* **2020**, *153*, No. 184311.
- (30) Oba, Y.; Tachikawa, M. Theoretical investigation of a positron binding to an aspartame molecule using the *ab initio* Multicomponent molecular orbital approach. *Int. J. Quantum Chem.* **2014**, *114*, 1146–1149.
- (31) Ono, K.; Oyamada, T.; Kita, Y.; Tachikawa, M. Theoretical analysis of the binding of a positron and pair-annihilation in fluorinated benzene molecules. *Eur. Phys. J. D* **2020**, *74*, No. 89.
- (32) Kita, Y.; Tachikawa, M. Positron binding properties for $F^-(H_2O)_n$ and $Cl^-(H_2O)_n$ ($n = 0-3$) clusters. *Chem. Phys. Lett.* **2009**, *482*, 201–206.
- (33) Chuang, S. Y.; Tao, S. J. Positron annihilation in amino acids and proteins. *J. Phys. Chem. A* **1974**, *78*, 1261–1265.
- (34) Koyanagi, K.; Kita, Y.; Tachikawa, M. Systematic theoretical investigation of a positron binding to amino acid molecules using the *ab initio* multi-component molecular orbital approach. *Eur. Phys. J. D* **2012**, *66*, No. 121.
- (35) Nummela, M.; Raebiger, H.; Yoshida, D.; Tachikawa, M. Positron binding properties of glycine and its aqueous complexes. *J. Phys. Chem. A* **2016**, *120*, 4037–4042.
- (36) Suzuki, K.; Sugiura, Y.; Takayanagi, T.; Kita, Y.; Tachikawa, M. Hydration effect on positron binding ability of proline: positron attachment induces proton-transfer to form zwitterionic Structure. *J. Phys. Chem. A* **2019**, *123*, 1217–1224.
- (37) Sugiura, Y.; Suzuki, K.; Koido, S.; Takayanagi, T.; Kita, Y.; Tachikawa, M. Quantum dynamics calculation of the annihilation spectrum for the positron-proline scattering. *Comput. Theor. Chem.* **2019**, *1147*, 1–7.
- (38) Charry, J. A.; Romero, J.; do Nascimento Varella, M. T.; Reyes, A. Calculation of positron binding energies of amino acids with the any-particle molecular-orbital approach. *Phys. Rev. A* **2014**, *89*, No. 052709.
- (39) González, S. A.; Aguirre, N. F.; Reyes, A. Theoretical investigation of isotope effects: The any-particle molecular orbital code. *Int. J. Quantum Chem.* **2008**, *108*, 1742–1749.
- (40) Ma, X.; Wang, L.; Yang, C. The dominant contributions of the inner valence electrons to the positron annihilation process in methanol. *Phys. Lett. A* **2014**, *378*, 1126–1129.
- (41) Ma, X.; Wang, L.; Yang, C. LOVO electrons: The special electrons of molecules in positron annihilation process. *J. Phys. Soc. Jpn.* **2014**, *83*, No. 054301.
- (42) Klasinc, L. Application of photoelectron spectroscopy to biologically active molecules and their constituent parts: III. Amino acids. *J. Electron Spectrosc. Relat. Phenom.* **1976**, *8*, 161–164.
- (43) Cannington, P. H.; Ham, N. S. He(I) and He(II) photoelectron spectra of glycine and related molecules. *J. Electron Spectrosc. Relat. Phenom.* **1983**, *32*, 139–151.
- (44) Green, D. G.; Gribakin, G. F. γ -Ray spectra and enhancement factors for positron annihilation with core electrons. *Phys. Rev. Lett.* **2015**, *114*, No. 093201.
- (45) Swann, A. R.; Gribakin, G. F. Calculations of positron binding and annihilation in polyatomic molecules. *J. Chem. Phys.* **2018**, *149*, No. 244305.
- (46) Swann, A. R.; Gribakin, G. F. Positron binding and annihilation in alkane molecules. *Phys. Rev. Lett.* **2019**, *123*, No. 113402.
- (47) Crawford, O. H. Bound states of a charged particle in a dipole field. *Proc. Phys. Soc.* **1967**, *91*, 279–284.
- (48) Compagnon, I.; Hagemester, F. C.; Antoine, R.; Rayane, D.; Broyer, M.; Dugourd, P.; Hudgins, R. R.; Jarrold, M. F. Permanent electric dipole and conformation of unsolvated tryptophan. *J. Am. Chem. Soc.* **2001**, *123*, 8440–8441.
- (49) Mitroy, J.; Ivanov, I. A. Semiempirical model of positron scattering and annihilation. *Phys. Rev. A* **2002**, *65*, No. 042705.
- (50) Tachikawa, M.; Mori, K.; Nakai, H.; Iguchi, K. An extension of *ab initio* molecular orbital theory to nuclear motion. *Chem. Phys. Lett.* **1998**, *290*, 437–442.
- (51) Tachikawa, M.; Mori, K.; Suzuki, K.; Iguchi, K. Full variational molecular orbital method: Application to the positron-molecule complexes. *Int. J. Quantum Chem.* **1998**, *70*, 491–501.
- (52) Schmidt, M. W.; Baldrige, K. K.; Boatz, J. A.; Elbert, S. T.; Gordon, M. S.; Jensen, J. H.; Koseki, S.; Matsunaga, N.; Nguyen, K. A.; Su, S.; Windus, T. L.; Dupuis, M.; Montgomery, J. A., Jr General atomic and molecular electronic structures system. *J. Comput. Chem.* **1993**, *14*, 1347–1363.

(53) Gordon, M. S.; Schmidt, M. W. *Theory and Applications of Computational Chemistry: The First Forty Years*; In Dykstra, C. E.; Frenking, G.; Kim, K. S.; Scuseria, G. E., Eds.; Elsevier: Amsterdam, 2005; Chapter 41, pp 1167–1189.

(54) Obara, S.; Saika, A. Efficient recursive computation of molecular integrals over Cartesian Gaussian functions. *J. Chem. Phys.* **1986**, *84*, 3963.

(55) Tachikawa, M.; Osamura, Y. Simultaneous optimization of exponents, centers of Gaussian-type basis functions, and geometry with full-configuration interaction wave function: Application to the ground and excited states of hydrogen molecule. *J. Chem. Phys.* **2000**, *113*, 4942.

(56) Wolcyrz, M. M.; Strasburger, K.; Chojnacki, H. Two-photon annihilation rate of the positronic HCN molecule. *Mol. Phys.* **2013**, *111*, 345–352.